HHS Public Access

Author manuscript

Dev Biol. Author manuscript; available in PMC 2017 January 15.

Published in final edited form as:

Dev Biol. 2016 January 15; 409(2): 382–391. doi:10.1016/j.ydbio.2015.11.024.

Prorenin receptor is critical for nephron progenitors

Renfang Song[a], **Graeme Preston**[a], **Laura Kidd**[a], **Daniel Bushnell**[b], **Sunder Sims-Lucas**[b], **Carlton M. Bates**[b], and **Ihor V. Yosypiv**[a,*]

[a]Department of Pediatrics, Department of Pathology, Tulane University School of Medicine, New Orleans, LA, 70112, USA

[b]Department of Pediatrics, University of Pittsburgh School of Medicine, Pittsburgh, PA 15201, USA

Abstract

Deficient nephrogenesis is the major factor contributing to renal hypoplasia defined as abnormally small kidneys. Nephron induction during kidney development is driven by reciprocal interactions between progenitor cells of the cap mesenchyme (CM) and the ureteric bud (UB). The prorenin receptor (PRR) is a receptor for renin and prorenin, and an accessory subunit of the vacuolar proton pump H^+-ATPase. Global loss of *PRR* is lethal in mice and *PRR* mutations are associated with a high blood pressure, left ventricular hypertrophy and X-linked mental retardation in humans. To circumvent lethality of the ubiquitous *PRR* mutation in mice and to determine the potential role of the PRR in nephrogenesis, we generated a mouse model with a conditional deletion of the *PRR* in $Six2^+$ nephron progenitors and their epithelial derivatives ($Six2^{PRR-/-}$). Targeted ablation of *PRR* in $Six2^+$ nephron progenitors caused a marked decrease in the number of developing nephrons, small cystic kidneys and podocyte foot process effacement at birth, and early postnatal death. Reduced congenital nephron endowment resulted from premature depletion of nephron progenitor cell population due to impaired progenitor cell proliferation and loss of normal molecular inductive response to canonical Wnt/β-catenin signaling within the metanephric mesenchyme. At 2 months of age, heterozygous $Six2^{PRR+/-}$ mice exhibited focal glomerulosclerosis, decreased kidney function and massive proteinuria. Collectively, these findings demonstrate a cell-autonomous requirement for the PRR within nephron progenitors for progenitor maintenance, progression of nephrogenesis, normal kidney development and function.

Keywords

Kidney development; nephron progenitor cells; nephrogenesis; prorenin receptor; renal hypodysplasia; proteinuria

[*]**Corresponding Author**: Ihor V. Yosypiv, M.D., Associate Professor, Department of Pediatrics, SL-37, Tulane University Health Sciences Center, 1430 Tulane Avenue, New Orleans, LA 70112, Tel: (504) 988-5377, Fax: (504) 988-1852, iiosipi@tulane.edu.

Statement of Competing Financial Interests

Nothing to disclose.

Introduction

Kidney development is driven by reciprocal inductive interactions between a multipotent, self-renewing $Six2^+$;$Cited1^+$ progenitor cells of the cap mesenchyme (CM) and the ureteric bud (UB) (Kobayashi et al., 2008). CM cells are continuously induced during metanephric organogenesis to condense around the surface of the UB tips and form pre-tubular aggregates (PTAs). PTAs undergo a mesenchyme to epithelial transition (MET) to sequentially form renal vesicles (RVs), comma- and S-shaped bodies (SBs), and, ultimately, most components of the mature nephrons, including the glomerulus, proximal tubule, loop of Henle and distal tubule (Little and McMahon, 2012). Although reduced nephron endowment has significant clinical implications such as renal hypoplasia, proteinuria, a limited capacity for kidney repair after injury, susceptibility to subsequent hypertension and chronic kidney disease (CKD), the mechanisms that determine final nephron number in health and disease are not well understood (Bertram et al., 2011).

The prorenin receptor (PRR) is a receptor for prorenin and renin encoded by the *ATP6AP2* (*ATPase-associated protein2*) gene (subsequently referred to as *PRR*) located on the × chromosome in humans (Nguyen et al., 2002). PRR is also an accessory protein of the vacuolar proton pump H^+-ATPase (Ludwig et al., 1998). H^+-ATPases are expressed in intracellular compartments of virtually all cell types and play important roles in protein trafficking and degradation *via* acidification of intracellular organelles (Forgac, 2007). In the intercalated cells of the collecting duct, H^+-ATPase is present at the plasma membrane where it is important for urine acidification (Wagner et al., 2004). Global *PRR* knockout is lethal in mice, indicating an essential role of the PRR in embryonic development (Sihn et al., 2013). In humans, *PRR* mutations are associated with a high blood pressure, left ventricular hypertrophy and X-linked mental retardation (Hirose et al., 2009; Hirose et al., 2011, Ramser et al., 2005). Recent data demonstrate that PRR is critical for normal kidney development and function. In this regard, *PRR* deletion in mice podocytes using the *Nphs2* promoter results in massive foot process effacement, proteinuria and nephrotic syndrome (Oshima et al., 2011). *PRR* ablation in the UB using the *Hoxb7* promoter leads to kidney hypoplasia, polyuria and a reduced capacity to acidify the urine (Song et al., 2013). However, the role of PRR in nephron progenitors remains unknown.

Here, we demonstrate that conditional inactivation of the *PRR* in $Six2^+$ nephron progenitors in mice results in small cystic kidneys at birth. We show that nephron progenitor population is depleted due to reduced cell proliferation and enhanced apoptosis, leading to fewer nephrons caused by impaired MET. Subsequently, $Six2^{PRR+/-}$ mice develop evidence of glomerular kidney disease with focal glomerulosclerosis, proteinuria and decreased kidney function. Collectively, these findings demonstrate a cell-autonomous requirement for the PRR within nephron progenitors for maintenance of progenitor cell pool, progression of nephrogenesis, normal kidney development and function.

Materials and Methods

Conditional Deletion of *PRR* from Nephron Progenitors

PRR-floxed mice were provided by Dr. Atsuhiro Ichihara (Keio University, Tokyo, Japan) (Oshima et al., 2011). To delete *PRR* conditionally in the CM and its epithelial derivatives, we used the *Six2GFPCre TGC* transgenic mice, which drives Cre expression in nephron progenitors (Kobayashi et al., 2008), and a floxed allele of the *PRR*. The resulting $Six2^{Cre+}/PRR^{flox/flox}$ mice represent nephron progenitor-specific *PRR*- knockout mice ($Six2^{PRR-/-}$). Control mice consisted of $PRR^{flox/flox}$ littermates ($Six2^{PRR+/+}$). All experiments involving mice were approved by Tulane Institutional Animal Care and Use Committee.

Quantitative Reverse-transcription Polymerase Chain Reaction (qRT-PCR)

qRT-PCR was performed in the Mx3000P equipment (Stratagene, La Jolla, CA) using MxPro QPCR software (Stratagene) as previously described (Song et al., 2013). mRNA was extracted from snap-frozen E12.5 and E18.5 $Six2^{PRR-/-}$ and control kidneys (E15.5 kidneys were pooled, E18.5- n=3 mice per group). The quantity of each target mRNA was normalized by that of GAPDH mRNA expression. RNA samples were analyzed in triplicates in each run. PCR reaction was performed twice.

Immunohistochemistry and Histopathology

Kidneys were fixed in 4% PFA at 4° C and paraffin embedded. Immunostaining was performed by the immunoperoxidase technique using 4-μm sections with Vectastain Elite kit (Vector Laboratories, Burlingame, CA). Primary antibodies included anti-PRR (1:200, Santa Cruz), anti-Lhx1 (1:10, developmental studies hybridoma bank), anti-Lef1 (1:100, cell signaling), anti-Jagged1 (1:100, Santa Cruz), anti-Sall1 (1:100, Abcam), anti-Pax2 (1:100, Invitrogen), anti-WT1 (1:100, Abcam), anti-active β-catenin (ABC, Millipore, 1:400), anti-Six2 (1:100, Proteintech) and Lotus Tetragonolobus Lectin (LTL) (1:400, Vector Laboratories). Whole intact E13.5 metanephroi from $PRR^{Six2-/-}$ and control mice (n=10 kidneys per genotype) were processed for the whole mount immunofluorescence using anti-cytokeratin antibody (1:200, Sigma) and the number of UB tips was counted. For immunofluorescence studies, secondary antibodies were detected with Alexa Fluor dyes (Invitrogen). Specificity of immunostaining was documented by the omission of the primary antibody. Kidneys from P0 $Six2^{PRR-/-}$ and control mice (n=3 mice per group) were cut in the longitudinal midplane, processed through the paraffin, and embedded on the cut surface. Kidneys were sectioned at 4-μm and stained with hematoxylin and eosin. The number of nephrons in each of 3 consecutive sections adjacent to the longitudinal midplane was counted and the mean number of nephrons per section per kidney was calculated. To determine the number of Six2-positive structures, we examined the intensity of Six2 immunofluorescence in P0 kidney sections (n=3 mice per group) using Slide book 4.0 software (Intelligent Imaging Innovations, Denver, CO). All counts were performed in a blinded fashion. For electron microscopy, P0 kidney tissues stored in 3% glutaraldehyde were processed and embedded by the Department of Pathology, Tulane University. Ultimately, 60 nm sections were cut and imaged using a Hitachi H-7100 electron microscope.

In situ hybridization (ISH)

Section ISH was performed on E14.5 and P0 *Six2*$^{PRR-/-}$ and control kidneys as previously described (Song et al., 2013). Mouse full length probes for *Cited1*, *Wnt4*, *Pax8*, *Wnt9b*, *Bmp7*, *Etv4* were a kind gift from Drs. Alan Perantoni, Leif Oxburgh and Carl Bates. 3 embryonic kidneys per group per probe were examined.

Cell proliferation and apoptosis assays

Cell proliferation and apoptosis was examined in E13.5 and P0 kidney sections from *Six2*$^{PRR-/-}$ and control mice (n=3 mice per genotype, 3 sections per kidney) as previously described (Song et al., 2013). Anti-phospho-histone H3 (pH3) and anti-cleaved caspase-3 antibodies were used (Cell Signaling, Danvers, MA; 1:50). Nephron progenitors were visualized with anti-Six2 antibody and UBs/UB-derived epithelia with anti-cytokeratin antibody. The number of proliferating and apoptotic cells in nephron progenitors was normalized to the total number of Six2-positive cells in each kidney section. The number of Six2-positive cells was determined by Image J software (NIH).

Measurement of creatinine and albumin

Blood and urine was obtained from P60 *Six2*$^{PRR+/-}$ and control mice (n=4 mice per genotype). All urine specimens were collected at 8 am. Each mouse was placed in an individual clean dry cage with no bedding and a sheet of plastic wrap placed on the bottom until urine was produced (approximately 30 min). Urine that was not contaminated with fecal waste was collected into autoclaved Eppendorf tubes and frozen at −20°C. Plasma and urine creatinine was measured by HPLC with picric acid (Jaffe method). Urinary albumin excretion was determined using the Albuwell ELISA kit (Exocell, Philadelphia, PA).

Fluorescence-Activated Cell Sorting (FACS)

E15.5 kidneys from *Six2*$^{PRR-/-}$ (*Six2*$^{Cre+}$/*PRR*$^{flox/flox}$) and control (*Six2*$^{Cre+}$/*PRR*$^{+/+}$) mice were digested in 0.25% Trypsin for 1 min at 37°C, dissociated by repetitive pipetting and resuspended in PBS containing 2% FBS and 10 mM EDTA. The resuspended cells were filtered through 40 μm nylon cell membrane (BD Falcon) and kept on ice until FACS. The GFP^{+} cells were isolated using FACS Vantage and data were subsequently analyzed with Diva software v.5.02 (Becton Dickinson). RNA was isolated using Absolutely RNA Nanoprep kit (Stratagene). qRT-PCR was performed to confirm elimination of *PRR* in FACS-isolated Six2+ cells from pooled *Six2*$^{PRR-/-}$ kidneys. For ABC immunofluorescence and CM differentiation studies of FACS-isolated CM cells, E15.5 kidneys were digested with collagenase A (25 mg/10 ml PBS) and pancreatin (100mg/10ml PBS) at 37 °C for 15 minutes.

ABC immunofluorescence and CM differentiation assay

FACS-isolated *Six2*$^{Cre+}$/*PRR*$^{flox/flox}$ and *Six2*$^{Cre+}$/*PRR*$^{+/+}$ cells from E15.5 kidneys were grown on Matrigel-coated 8 chamber slides (20,000 cells/chamber) in DMEM/F12 medium with 10% FBS. After 24h, cells were stained with anti-ABC antibody (Millipore, 1:400) followed by secondary antibody (Alexa Fluor 555). For CM differentiation assay, 1×10^5 FACS-isolated *Six2*$^{Cre+}$/*PRR*$^{flox/flox}$ and *Six2*$^{Cre+}$/*PRR*$^{+/+}$ cells were aggregated and grown

on transwell filters placed on DMEM/F12 medium with 10% FBS in the presence of glycogen synthase kinase 3 inhibitor 6-bromoindirubin-3'-oxime (BIO, 4 μM) or DMSO (control) for the first 24h followed by medium with DMSO for the subsequent 24h, as described before (Park et al., 2012). Cells were fixed in 4% PFA for 10 min and stained with an antibody against E-cadherin (indicator of epithelialization, 1:200, BD Biosciences) and Lef1 (indicator of canonical Wnt signaling) (Filali et al., 2002). Treatments with BIO were performed on three separate pools of FACS-isolated cells.

3D Reconstruction and Analysis

3D reconstructions of E12.5 control and *Six2*$^{PRR-/-}$ developing nephrons and ureteric trees were performed as described (Sims-Lucas et al., 2009). Briefly, image layers were created from projected serial H&E stained sections (4 μm) by tracing around capsules of nephrogenic structures which were classified as RVs, comma-shaped bodies, SBs, immature glomeruli or the ureteric tree based on the morphology of the structures (Stereoinvestigator, Microbrightfield, MBF, VT). Traced layers were aligned and rendered into a 3D graphical reconstruction, from which nephron structure and ureteric tip number as well as total kidney, nephron structure, and ureteric surface areas and volumes were determined.

Statistics

Statistical analyses were carried out upon all biologic replicates with Student's t test or a one-way ANOVA, followed by Bonferroni test. Data are presented as Mean±SEM. A p value of <0.05 was considered statistically significant.

Results

PRR is required within mesenchymal progenitors for progression of nephrogenesis

To examine the role of PRR in nephron progenitors, we removed *PRR* from the CM using the *Six2TGC* line in combination with a floxed allele of the *PRR*. Mutant mice were born at normal Mendelian ratios but died within 48 hours from birth. qRT-PCR revealed a 71% decrease in PRR mRNA levels in Six2$^+$ cells FACS-isolated from E15.5 *Six2*$^{PRR-/-}$ compared with control kidneys (0.29±0.01 vs. 1.0±0, $p<0.001$) (Fig. 1). On E15.5, double immunostaining of PRR and cytokeratin revealed reduced PRR expression in the mesenchyme in *Six2*$^{PRR-/-}$ mice (Fig. 1).

On E12.5, *Six2*$^{PRR-/-}$ kidneys appeared grossly similar to controls on 3D reconstruction (Fig. 1). Mean mutant and control kidney and UB tree volumes were not significantly different (Table 1). However, developing glomeruli volume (relative to kidney volume) and average size were reduced in mutants. While RV number was not statistically different, the number of comma- and SBs was reduced in mutants (Fig. 1, Table 1). Thus, it appears that nascent nephrons reach RV stage, but do not develop beyond in *Six2*$^{PRR-/-}$ mutants. Because of this, nephron structure volume compared to the total kidney volume is reduced in mutants at this stage.

On E13.5, mutant kidneys had reduced size and less developed epithelial structures (Fig. 2). In control kidneys, nephrogenesis was active and several vesicles and comma-shaped

nephrons were apparent (Fig. 2). In contrast, *Six2*$^{PRR-/-}$ mutants had few vesicles and comma-shaped nephron structures apparent (Fig. 2). UB branching was reduced at this stage of kidney development (28±3.5 vs. 41±1.6, p<0.001), likely secondary to decreased nephrogenesis (Fig. 2).

PRR promotes nephrogenesis through progenitor maintenance

We next investigated the early molecular responses to inductive signaling within the metanephric mesenchyme resulting from *PRR* deletion. The transition of responding progenitors to PTAs and RVs is directed by Wnt4, Fgf8, Pax8, and Lhx1 which act downstream of Wnt9b (Valerius et al., 2002; Stark et al., 1994; Grieshammer et al., 2005). Lef1 and Jagged1 (Jag1) represent additional RV markers.[15] Hence, these markers enable a detailed molecular analysis of the inductive steps of nephrogenesis program. ISH demonstrated apparent reduction in *Wnt4 and Pax8* expression in E13.0 *Six2*$^{PRR-/-}$ compared to control kidneys (Fig. 3). Expression pattern of *Wnt9b* (in the UB stalk) was not altered (Fig. 3). Immunofluorescence demonstrated decreased number of Lef1 (2.2±0.3 vs. 10±1.1, p<0.001), Jag1 (3.1±0.7 vs. 15±2.1, p<0.001) and Lhx1 (8±1.2 vs. 21±2.6, p<0.001)-positive structures in E14.5 mutant compared to control kidneys (Fig. 3). qRT-PCR showed reduced expression of *Wnt4, Fgf8, Pax8, Lhx1, Lef1, Jag1* and *Fgf20* (p<0.001), and no change in *Wnt9b* and *Bmp7* mRNA levels in whole E14.5 *Six2*$^{PRR-/-}$ metanephroi compared to controls (Fig. S1). Thus, a greatly reduced inductive and differentiation response was observed in *Six2*$^{PRR-/-}$ mutants in spite of unaltered *Wnt9b* expression.

To test the hypothesis that decreased nephrogenesis in *Six2*$^{PRR-/-}$ mutants is due, in part, to premature depletion of nephron progenitors, we examined the expression of Six2, Cited1 and Sall1, markers of CM cells with self-renewing capacity (Kobayashi et al., 2008; Carroll et al., 2005; Mugford et al., 2009; Brown et al., 2013). *Cited1, Six2 and Sall1* mRNA levels were reduced in *Six2*$^{PRR-/-}$ whole mutant kidneys (Fig. S1). Consistent with qRT-PCR data, Cited1, Six2 and Sall1 immunostaining in the CMs of mutants was substantially decreased (Fig. 3, Fig. S1). Quantification of fluorescence intensity of Cited1, Six2 or Sall1 immunostaining per kidney section demonstrated ~50-fold reduction in Cited1, ~5-fold reduction in Six2 and ~3-fold reduction in Sall1 expression in mutant compared to control kidneys (Cited1: $2.69\times10^4\pm4.2\times10^3$ vs. $1.38\times10^6\pm9.0\times10^4$, p<0.001; Cited1/DAPI: 0.06±0.01 vs. 2.7±0.16, p<0.01; Six2: $1.28\times10^6\pm9.7\times10^4$ vs. $8.08\times10^6\pm8.8\times10^4$, p<0.001; Six2/DAPI: 3.5±0.6 vs. 15.5±1.0, p<0.01; Sall1: $2.67\times10^6\pm4.6\times10^4$ vs. $8.06\times10^6\pm9.2\times10^4$, p<0.05; Sall1/DAPI: 3.2±0.5 vs. 6.2±0.5, p<0.05). These findings demonstrate that CM PRR maintains Cited1$^+$, Six2$^+$ and Sall1$^+$ progenitor cells with most pronounced effect on the Cited1$^+$ subcompartment of the nephron progenitor pool. It is conceivable that premature loss of Cited1$^+$ cells with relative persistence of Six2$^+$ population may account for premature commitment of progenitors to nephron differentiation in mutants. Collectively, reduced early inductive response observed in *Six2*$^{PRR-/-}$ mutants may result from precocious depletion of the progenitor population and premature commitment of progenitors to nephron differentiation.

Since BMP7 and Fgf20 promote/maintain progenitor self-renewal (Barak et al., 2012; Brown et al., 2013), we next tested whether premature depletion of the progenitor population in *Six2*$^{PRR-/-}$ mutants is due to reduced expression/activity of BMP7 or Fgf20. Consistent with qRT-PCR data, expression pattern of *Bmp7* mRNA in the CM was unaltered (Fig. S1). Given that Bmp7 signaling *via* phospho-Smad1/5 (pSmad1/5) was shown to be required for transition of progenitors from the Cited1^{+}/Six2^{+} to Cited1 $^{-}$/Six2^{+} compartment of the CM, thereby sensitizing progenitor cells to inductive effects of Wnt9b (Brown et al., 2013), we next investigated whether premature depletion of Cited1^{+} cells in *Six2*$^{PRR-/-}$ mutants is due to increased pSmad1/5 expression in the CM. pSmad1/5 expression in the CM of mutant kidneys was increased (Fig. S1). Given that *Fgf20* mRNA levels were reduced in the mutant kidney, we next determined the expression of *Etv4*, which correlates with Fgf activity (Carroll et al., 2005; Barak et al., 2012). *Etv4* expression was reduced in mutant compared to control kidneys (Fig. S1). Thus, increased pSmad expression and reduced *Sall1*/*Fgf20* expression and *Fgf* signaling *via Etv4* in the CM may contribute to precocious depletion of the progenitor cells in *Six2*$^{PRR-/-}$ kidneys.

Since progenitor cell-specific removal of β-catenin inhibits nephrogenesis (Park et al., 2007) and PRR activates Wnt co-receptor LRP, thus promoting canonical *Wnt*/β-catenin signaling (Cruciat et al., 2010), we next examined whether expression of active form of β-catenin protein (ABC) dephosphorylated on $^{Ser}37$ or $^{Thr}41$ is reduced in *Six2*$^{PRR-/-}$ mutant kidneys. We found that ABC expression in the CM of *Six2*$^{PRR-/-}$ mutants was reduced (Fig. 4). In addition, ABC immunofluorescence was decreased in Six2^{+} cells FACS-isolated from E15.5 *Six2*$^{PRR-/-}$ mutant kidneys compared with controls (Fig. 4). Quantification of fluorescence intensity of ABC immunostaining demonstrated ~5-fold reduction in ABC expression in mutant compared to control cells (ABC: $1.38\times10^{6}\pm9.0\times10^{4}$ vs. $4.88\times10^{5}\pm7.0\times10^{4}$, $p<0.01$; ABC/DAPI: 1.49±0.18 vs. 3.3±0.29, $p<0.01$). To determine the role of β-catenin signaling downstream of the CM PRR in MET, we induced Wnt/β-catenin pathway-activated MET in Six2^{+} cells FACS-isolated from E15.5 *Six2*$^{Cre+}$/*PRR*$^{flox/flox}$ and *Six2*$^{Cre+}$/*PRR*$^{+/+}$ kidneys with BIO which mimics canonical Wnt signaling response by inhibiting GSK-3β-mediated β-catenin degradation. DMSO (control)-treated *Six2*$^{Cre+}$/*PRR*$^{+/+}$ cells expressed E-cadherin, Lef1 and formed multicellular structures, indicative of active MET (Fig. 4). In contrast, *Six2*$^{Cre+}$/*PRR*$^{flox/flox}$ cells showed very weak E-cadherin/Lef1 expression, and failed to form multicellular structures, indicating that intact PRR signaling in nephron progenitor cells (NPC) is required for proper MET. Upon induction of β-catenin activity with BIO, E-cadherin, Lef1 expression and complexity of multicellular structures increased in both *Six2*$^{Cre+}$/*PRR*$^{+/+}$ and *Six2*$^{Cre+}$/*PRR*$^{flox/flox}$ cells compared to vehicle (DMSO)-treated controls (Fig. 4). However, induction of MET was attenuated in *Six2*$^{Cre+}$/*PRR*$^{flox/flox}$ compared to *Six2*$^{Cre+}$/*PRR*$^{+/+}$ cells. These data demonstrate that NPC PRR promotes MET *via* induction of canonical Wnt/β-catenin signaling in Six2^{+} NPC.

PRR regulates nephron progenitor proliferation

To identify the cellular mechanisms by which *PRR* deficiency in the CM could deplete nephron progenitor pool and attenuate the inductive response, we examined cell proliferation and apoptosis in Six2^{+} compartment of the CM on E13.5. The number of pH3-positive proliferating cells in the CM per kidney section was lower in E13.5 *Six2*$^{PRR-/-}$

compared to control kidneys (8±1.6 vs. 27±2.5, p<0.001) while the number of caspase 3-positive apoptotic cells did not differ (2.5±1 vs. 2.2±0.8, p=0.83) (Fig. 5). These findings indicate that progenitor depletion in *Six2*$^{PRR-/-}$ mice may be caused by proliferation defects.

Targeted *PRR* deletion results in small cystic kidneys at birth and podocyte foot process effacement

Newborn (P0) *Six2*$^{PRR-/-}$ mice had smaller kidney size (kidney length: 870±21 vs. 1295±23 μm, p<0.001) (Fig. 6). On P0, body weight did not differ in mutant and control mice (1.21±0.06 vs. 1.23±0.05 g, p=0.92). In contrast, kidney weight (7.7±0.6 vs. 12.1±0.6 mg, p<0.01) was lower in mutants than in controls. Histological examination revealed that mutant kidneys have normal shape and are architecturally organized into cortex, medulla and papilla with radially arranged collecting system. Mutant kidneys lack a well-defined nephrogenic zone, have thin cortex, many cysts in the cortex and outer medulla, and decreased mean number of nephrons per section per kidney compared to controls (47±4.4 vs. 190±3.8, p<0.001) (Fig. 6). To determine whether deletion of *PRR* from nephron progenitors arrests nephrogenesis in a defined stage of nephron maturation, we counted nephron generation numbers in mutant and control kidneys on P0. All stages of nephron development were reduced in mutants compared to controls, suggesting that decreased number of more mature forms in mutants is due to reduced nephron induction (Fig. 6).

To define the effect of *PRR* deletion in the CM on nephron progenitors, nephron induction and segmentation during later stages of nephrogenesis, we performed ISH and immunofluorescence for markers specific for the CM and developing nephron structures on P0. ISH showed presence of *Cited1* mRNA expression in the nephrogenic zone in controls and complete absence of its expression in the nephrogenic zone in mutants (Fig. S2). These findings demonstrate an important role for nephron progenitor PRR in the maintenance of Cited1^{+} population and suggest that persistent reduction in nephron number in *PRR* mutants at birth is due to precocious depletion of progenitor pool. There was also a marked reduction in staining for WT1-positive glomeruli, lotus tetragonolobus Lectin (LTL)-expressing tubules of proximal tubule origin and Pax2/Jag1-positive RVs in mutants (Fig. S2). These data indicate that nephron induction and specification of proximal nephron segments (which arise from nephron progenitors) is impaired in *Six2*$^{PRR-/-}$ mutants at birth. Given reduced expression of podocyte marker WT1 in mutants, we performed electron microscopy (EM) to assess podocyte ultrastructure on P0. EM demonstrated podocyte foot process effacement in *Six2*$^{PRR-/-}$ mutants (Fig. 7). Thus, loss of *PRR* from nephron progenitors results in podocyte foot process effacement, a hallmark of glomerular injury leading to proteinuria.

PRR deletion results in a decreased cell proliferation and an increased cell apoptosis at birth

To identify the cellular mechanisms accounting for small cystic kidneys observed in *Six2*$^{PRR-/-}$ mutants at birth, we examined cell proliferation and apoptosis in the Six2^{+} compartment of the CM on P0. Quantification of fluorescence intensity of phosphohistone H3 (pH3) and activated caspase-3 (Casp3) in the Six2^{+} compartment revealed that the ratio of proliferating/Six2-positive cells was reduced (0.054±0.006 vs. 0.096±0.01, p<0.05) and of apoptotic/Six2-positive cells per kidney section was increased (1.08±0.06 vs.

0.007±0.001, p<0.001) in mutants compared with controls (Fig. S3). These findings demonstrate that loss of *PRR* in nephron progenitors results in impaired cell proliferation and survival in $Six2^{+}$ compartment of the CM during later stages of nephrogenesis, leading to congenitally small cystic kidneys.

Reduced *PRR* gene dosage in nephron progenitors results in proteinuric kidney disease

Because $Six2^{PRR-/-}$ mice did not survive beyond the first 48 hours of life, we evaluated the functional consequences of reduced *PRR* gene dosage in $Six2^{PRR+/-}$ mice at 2 months of age. Kidney weight was reduced in $Six2^{PRR+/-}$ compared to control mice (0.288±0.01 vs. 0.408±0.02 g, p<0.001) (Fig. 7). Histological analysis of $Six2^{PRR+/-}$ kidneys demonstrated focal glomerulosclerosis (Fig. 7). Serum creatinine levels and urinary albumin excretion were increased in $Six2^{PRR+/-}$ mice compared to Cre-negative controls (Fig. 7). These data indicate that reduced *PRR* gene dosage in nephron progenitors results in histologic glomerular injury, proteinuric kidney disease and renal dysfunction. Taken with the histologic data showing podocyte effacement in $Six2^{PRR-/-}$ mice at birth, the podocyte foot process effacement is probably responsible, in part, for proteinuria in $Six2^{PRR+/-}$ mice at 2 months of age. These findings are in keeping with previously published reports in which podocyte-specific loss of *PRR* results in proteinuric kidney disease due to abnormal podocyte function (Oshima et al., 2011).

Discussion

We demonstrate that nephron progenitor PRR is essential for the maintenance of progenitor cells of the CM and the induction of nephrogenesis during metanephric kidney development. Conditional deletion of *PRR* in nephron progenitors causes premature depletion of NPC pool resulting in decreased mesenchyme to epithelial transition required for later stages of nephron formation. Reduced nephron endowment and small cystic kidneys are related to impaired progenitor cell proliferation and loss of normal molecular inductive response to canonical Wnt/β-catenin signaling that occur early in kidney development. Postnatally, heterozygous $Six2^{PRR+/-}$ animals develop focal glomerulosclerosis and proteinuric kidney disease.

The balance of NPC self-renewal and differentiation into nephrons ultimately determines nephron endowment (Little and McMahon, 2012). Premature depletion of progenitors during kidney development results in renal hypoplasia, a common cause of pediatric end-stage renal disease and a risk factor for hypertension (Bertram et al., 2011). Six2, Eya1, Osr1, Pax2, Sall1, Bmp7, Fgf2, Fgf9, Fgf20 and Wnt signaling pathways are essential in regulating the balance between self-renewal and differentiation of progenitor cells throughout nephrogenesis to generate sufficient number of nephrons by term birth in humans (Brown et al., 2013; Kanda et al., 2014; Barak et al., 2012; Brown et al., 2011; Blank et al., 2009; Self et al., 2006). UB-derived Wnt9b is a primary inductive signal required to initiate the transition of NPC of the CM toward nephron differentiation *via* the stabilization of β-catenin within the CM (Grieshammer et al., 2005; Xu et al., 2014). While the least differentiated nephron progenitor compartment is marked by Cited1, Six2 and Sall1, Fgf8, Pax8, Wnt4 and Lhx1 represent the earliest markers that demarcate the

transition of nephron progenitors responding to Wnt9b signaling to PTAs and RVs (Valerius et al., 2002; Stark et al., 1994; Grieshammer et al., 2005).

In the mouse kidney, PRR mRNA and protein are detected from E12.5 (Song et al., 2013b). PRR mRNA is expressed in the intact UBs isolated from E11.5 wild-type mouse kidneys (Song et al., 2013a). PRR immunostaining is present in the UB and the CM on E13.5 (Song et al., 2013a). In this study, we found that PRR maintains nephron progenitors and promotes differentiation of nascent nephrons by regulating the expression of key genes critical for both populations. The expression of Six2, Cited1 and Sall1, which are essential for maintaining stemness of the nephrogenic niche (Kobayashi et al., 2008; Mugford et al., 2009; Brown et al., 2013), was reduced in *PRR* mutants. The early loss of *Cited1*$^{+}$ cells in our study may indicate reduced survival of the progenitors and/or their premature commitment to nephron induction (Mugford et al., 2009). The observed depletion of Cited1^{+} population in *PRR* mutants may be due to increased signaling *via* pSmad, previously shown to be required for transition of progenitors to a distinct Six2^{+};Cited1- subcompartment in which cells are sensitized to inductive effects of canonical *Wnts* (Mugford et al., 2009). Reduced nephrogenesis in *PRR* mutants may be also attributed to decreased expression of *Sall1* and *Fgf20* (and *Fgf20* signaling *via Etv4*) in the mesenchyme. This possibility is supported by similarity in renal phenotype in *Six2*$^{\mathrm{PRR}-/-}$ mice and in mice with conditional loss of *Sall1* in S*ix2*-positive progenitors or in *Fgf20*$^{\beta\mathrm{Gal}/\beta\mathrm{Gal}}$;*Fgf9*$^{+/-}$ compound mutants. Both *Sall1* and *Fgf20*$^{\beta\mathrm{Gal}/\beta\mathrm{Gal}}$;*Fgf9*$^{+/-}$ mutants have small dysplastic kidneys at birth due to depletion of nephron progenitors and premature cessation of nephrogenesis (Brown et al., 2013; Kanda et al., 2014).

PRR may also control nephrogenesis through the canonical *Wnt/* β-catenin signaling. In this regard, inhibition of the *PRR* by small inhibitory RNA (siRNA) in HEK293T cells *in vitro* or by the *PRR* antisense morpholino in *Xenopus* embryos *in vivo* decreases luciferase reporter activity stimulated by canonical *Wnt* signaling (Cruciat et al., 2010). Emerging evidence indicates that Wnt/β-catenin signaling regulates both NPC self-renewal and differentiation. The disparate responses (self-renewal vs. differentiation) are controlled, in part, by expression levels of Six2 (Karner et al., 2011; Park et al., 2012). In CM cells with high Six2 levels, Six2 forms complexes with β-catenin binding patners Tcf/Lef and prevents β-catenin from activating the expression of genes promoting differentiation (Park et al., 2012). In NPCs induced by a high dosage of Wnt9b, increased β-catenin levels reduce Six2 levels, resulting in upregulation of genes such as *Wnt4* and *Fgf8* which are essential for nephrogenesis (Karner et al., 2011; Park et al., 2012). In spite of unaltered expression pattern of *Wnt9b* in the UB of *Six2*$^{\mathrm{PRR}-/-}$ mutants in our study, we observed reduction in active β-catenin protein levels in the mutant CM and in Six2^{+} cells FACS-isolated from E15.5 *Six2*$^{\mathrm{PRR}-/-}$ mutant kidneys. Moreover, *Six2*$^{\mathrm{Cre}+}$/*PRR*$^{\mathrm{flox/flox}}$ cells showed weak E-cadherin/Lef1 expression, and failed to form multicellular structures. These findings provide strong evidence that β-catenin-dependent canonical Wnt signaling downstream of the PRR plays a central role in the initiation of MET (Valerius et al., 2002; Xu et al., 2014).

Finally, as H^{+}-ATPase subunit, PRR may be important for progenitor cell survival through maintenance of pH homeostasis. In this regard, conditional loss of the *PRR* from podocytes in mice causes downregulation of H^{+}-ATPase subunit expression, impaired acidification of

intracellular comparments, foot process effacement and proteinuria (Oshima et al., 2011). In our study, ablation of the *PRR* in nephron progenitors resulted in podocyte foot process effacement at birth and decrease in *PRR* gene dosage- in proteinuric kidney disease later in life. Thus, nephron progenitor PRR is essential for glomerular structure and function.

In summary, nephron progenitor PRR is essential for nephron development and renal function postnatally. We propose that PRR positively regulates targets in nephron progenitors, thereby maintaining stemness of nephron progenitor niche. Findings of small cystic kidneys and podocyte foot process effacement observed in *PRR* mutants at birth points to *PRR* as a potential candidate for future genetic screening studies in humans with renal hypoplasia, hypodysplasia and podocytopathy.

Supplementary Material

Refer to Web version on PubMed Central for supplementary material.

Acknowledgments

We thank Drs. Atsuhiro Ichihara and Andrew McMahon for providing $PRR^{flox/flox}$ and $Six2^{Cre+}$ mice, respectively. We thank Drs. Alan Perantoni, Leif Oxburgh, Carlton Bates and Thomas Carroll for providing the probes for ISH. This work was supported by R01-DK095748 (CMB) and the O'Brien Center P30 (DK079307).

References

1. Barak H, Huh SH, Chen S, Jeanpierre C, Martinovic J, Parisot M, Bole-Feysot C, Nitschké P, Salomon R, Antignac C, Ornitz DM, Kopan R. FGF9 and FGF20 maintain the stemness of nephron progenitors in mice and man. Dev Cell. 2012; (22):1191–1207. [PubMed: 22698282]
2. Bertram JF, Douglas-Denton RN, Diouf B, Hughson MD, Hoy WE. Human nephron number: implications for health and disease. Pediatr Nephrol. 2011; (26):1529–1533. [PubMed: 21604189]
3. Blank U, Brown A, Adams DC, Karolak MJ, Oxburgh L. BMP7 promotes proliferation of nephron progenitor cells via a JNK-dependent mechanism. Development. 2009; (136):3557–3566. [PubMed: 19793891]
4. Brown AC, Adams D, de Caestecker M, Yang X, Friesel R, Oxburgh L. FGF/EGF signaling regulates the renewal of early nephron progenitors during embryonic development. Development. 2011; (138):5099–5112. [PubMed: 22031548]
5. Brown AC, Muthukrishnan SD, Guay JA, Adams DC, Schafer DA, Fetting JL, Oxburgh L. Role for compartmentalization in nephron progenitor differentiation. Proc Natl Acad Sci U S A. 2013; (110): 4640–4645. [PubMed: 23487745]
6. Carroll TJ, Park JS, Hayashi S, Majumdar A, McMahon AP. Wnt9b plays a central role in the regulation of mesenchymal to epithelial transitions underlying organogenesis of the mammalian urogenital system. Dev Cell. 2005; (9):283–292. [PubMed: 16054034]
7. Cruciat CM, Ohkawara B, Acebron SP, Karaulanov E, Reinhard C, Ingelfinger D, Boutros M, Niehrs C. Requirement of prorenin receptor and vacuolar H+-ATPase-mediated acidification for Wnt signaling. Science. 2010; (327):459–463. [PubMed: 20093472]
8. Filali M, Cheng N, Abbott D, Leontiev V, Engelhardt JF. Wnt-3A/beta-catenin signaling induces transcription from the LEF-1 promoter. J Biol Chem. (36):33398–33410.
9. Forgac M. Vacuolar ATPases: rotary proton pumps in physiology and pathophysiology. Nat Rev Mol Cell Biol. 2007; (8):917–929. [PubMed: 17912264]
10. Grieshammer U, Cebrián C, Ilagan R, Meyers E, Herzlinger D, Martin GR. FGF8 is required for cell survival at distinct stages of nephrogenesis and for regulation of gene expression in nascent nephrons. Development. 2005; (132):3847–3857. [PubMed: 16049112]

11. Hirose T, Hashimoto M, Totsune K, Metoki H, Asayama K, Kikuya M, Sugimoto K, Katsuya T, Ohkubo T, Hashimoto J, Rakugi H, Takahashi K, Imai Y. Association of (pro)renin receptor gene polymorphism with blood pressure in Japanese men: the Ohasama study. Am J Hypertens. 2009; (22):294–299. [PubMed: 19131936]
12. Hirose T, Hashimoto M, Totsune K, Metoki H, Hara A, Satoh M, Kikuya M, Ohkubo T, Asayama K, Kondo T, Kamide K, Katsuya T, Ogihara T, Izumi S, Rakugi H, Takahashi K, Imai Y. Association of (pro)renin receptor gene polymorphisms with lacunar infarction and left ventricular hypertrophy in Japanese women: the Ohasama study. Hypertens Res. 2011; (34):530–535. [PubMed: 21228785]
13. Kanda S, Tanigawa S, Ohmori T, Taguchi A, Kudo K, Suzuki Y, Sato Y, Hino S, Sander M, Perantoni AO, Sugano S, Nakao M, Nishinakamura R. Sall1 maintains nephron progenitors and nascent nephrons by acting as both an activator and a repressor. J Am Soc Nephrol. 2014; (25): 2584–2595. [PubMed: 24744442]
14. Karner CM, Das A, Ma Z, Self M, Chen C, Lum L, Oliver G, Carroll TJ. Canonical Wnt9b signaling balances progenitor cell expansion and differentiation during kidney development. Development. 2011; (138):1247–1257. [PubMed: 21350016]
15. Kobayashi A, Valerius MT, Mugford JW, Carroll TJ, Self M, Oliver G, McMahon AP. Six2 defines and regulates a multipotent self-renewing nephron progenitor population throughout mammalian kidney development. Cell Stem Cell. 2008; (3):169–181. [PubMed: 18682239]
16. Little MH, McMahon AP. Mammalian kidney development: principles, progress, and projections. Cold Spring Harb Perspect Biol. 2012; (4):1–18.
17. Ludwig J, Kerscher S, Brandt U, Pfeiffer K, Getlawi F, Apps DK, Schägger H. Identification and characterization of a novel 9.2-kDa membrane sector-associated protein of vacuolar proton-ATPase from chromaffin granules. J Biol Chem. 1998; (273):10939–10947. [PubMed: 9556572]
18. Mugford JW, Yu J, Kobayashi A, McMahon AP. High-resolution gene expression analysis of the developing mouse kidney defines novel cellular compartments within the nephron progenitor population. Dev Biol. 2009; (333):312–323. [PubMed: 19591821]
19. Nguyen G, Delarue F, Burcklé C, Bouzhir L, Giller T, Sraer JD. Pivotal role of the renin/prorenin receptor in angiotensin II production and cellular responses to renin. J Clin Invest. 2002; (109): 1417–1427. [PubMed: 12045255]
20. Oshima Y, Kinouchi K, Ichihara A, Sakoda M, Kurauchi-Mito A, Bokuda K, Narita T, Kurosawa H, Sun-Wada GH, Wada Y, Yamada T, Takemoto M, Saleem MA, Quaggin SE, Itoh H. Prorenin receptor is essential for normal podocyte structure and function. J Am Soc Nephrol. 2011; (22): 2203–2212. [PubMed: 22052048]
21. Park JS, Valerius MT, McMahon AP. Wnt/beta-catenin signaling regulates nephron induction during mouse kidney development. Development. 2007; (134):2533–2539. [PubMed: 17537789]
22. Park JS, Ma W, O'Brien LL, Chung E, Guo JJ, Cheng JG, Valerius MT, McMahon JA, Wong WH, McMahon AP. Six2 and Wnt regulate self-renewal and commitment of nephron progenitors through shared gene regulatory networks. Dev Cell. 2012; (3):637–651. [PubMed: 22902740]
23. Ramser J, Abidi FE, Burckle CA, Lenski C, Toriello H, Wen G, Lubs HA, Engert S, Stevenson RE, Meindl A, Schwartz CE, Nguyen G. A unique exonic splice enhancer mutation in a family with X-linked mental retardation and epilepsy points to a novel role of the renin receptor. Hum Mol Genet. 2005; (14):1019–1027. [PubMed: 15746149]
24. Self M, Lagutin OV, Bowling B, Hendrix J, Cai Y, Dressler GR, Oliver G. Six2 is required for suppression of nephrogenesis and progenitor renewal in the developing kidney. EMBO J. 2006; (25):5214–5228. [PubMed: 17036046]
25. Sihn G, Burckle C, Rousselle A, Reimer T, Bader M. (Pro)renin receptor: subcellular localizations and functions. Front Biosci. 2013; (5):500–508.
26. Sims-Lucas S, Argyropoulos C, Kish K, McHugh K, Bertram JF, Quigley R, Bates CM. Three-dimensional imaging reveals ureteric and mesenchymal defects in Fgfr2-mutant kidneys. J Am Soc Nephrol. 2009; 20(12):2525–2533. [PubMed: 19833900]
27. Song R, Preston G, Yosypiv IV. Ontogeny of the (pro)renin receptor. Pediatr Res. 5–10; (74)
28. Song R, Preston G, Ichihara A, Yosypiv IV. Deletion of the prorenin receptor from the ureteric bud causes renal hypodysplasia. PLoS ONE. 2013; (8):e63835. [PubMed: 23704941]

29. Stark K, Vainio S, Vassileva G, McMahon AP. Epithelial transformation of metanephric mesenchyme in the developing kidney regulated by Wnt-4. Nature. 1994; (372):679–683. [PubMed: 7990960]

30. Valerius MT, Patterson LT, Witte D, Potter SS. Microarray analysis of novel cell lines representing two stages of metanephric mesenchyme differentiation. Mech Dev. 2002; (112):219–232. [PubMed: 11850199]

31. Wagner CA, Finberg KE, Breton S, Marshansky V, Brown D, et al. Renal vacuolar H+-ATPase. Physiol Rev. 2004; (84):1263–1314. [PubMed: 15383652]

32. Xu J, Liu H, Park JS, Lan Y, Jiang R. Osr1 acts downstream of and interacts synergistically with Six2 to maintain nephron progenitor cells during kidney organogenesis. Development; (141): 1442–1452.

Highlights

- Conditional deletion of the prorenin receptor (*PRR*) in nephron progenitors in mice causes reduced nephron endowment and severe congenital bilateral renal hypodysplasia (RHD).
- RHD results from premature depletion of nephron progenitor cell pool, decreased nephrogenesis and secondary ureteric bud branching defects.
- Mechanistically, aberrant kidney development is due to impaired progenitor cell proliferation and loss of normal molecular inductive response to canonical Wnt/β-catenin signaling.
- Postnatally, heterozygous *Six2*$^{PRR+/-}$ animals develop focal glomerulosclerosis and proteinuric kidney disease.
- Nephron progenitor prorenin receptor (PRR) is essential for normal kidney development and function.

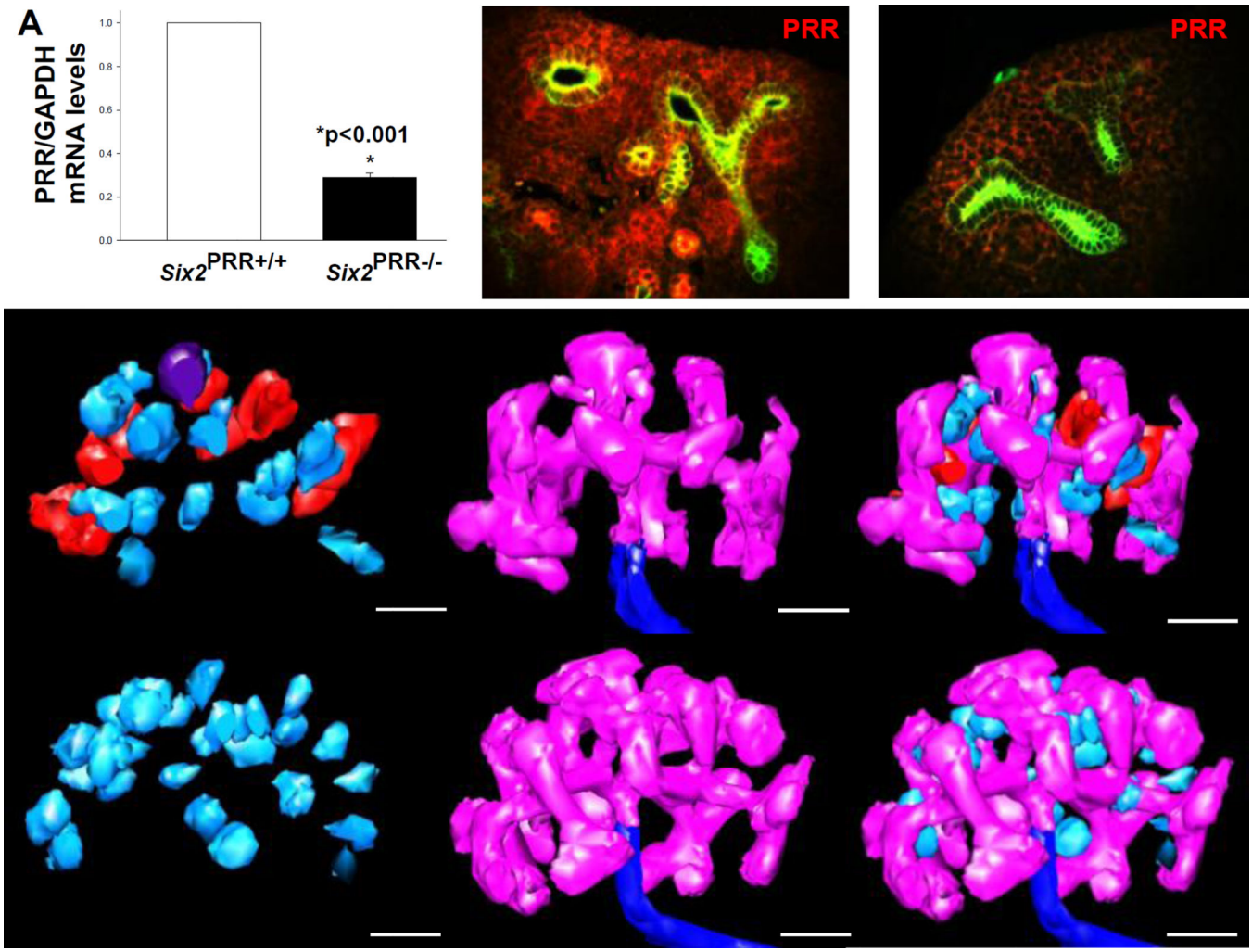

Figure 1. Nephron progenitor PRR is required for nephrogenesis

Efficiency of *Six2*-Cre-mediated *PRR* deletion. (A) PRR mRNA levels are reduced in Six2^{+} cells FACS-isolated from E15.5 *Six2*$^{PRR-/-}$ kidneys compared with controls. (B,C) PRR immunostaining (red) is reduced in the mesenchyme of *Six2*$^{PRR-/-}$ E15.5 kidneys. Ureteric buds (UB) are visualized with anti-pancytokeratin antibody (green staining). (D–I) 3D reconstruction of E12.5 kidneys demonstrates that mutant kidneys have no nephrons past the RV stage (light blue), while control kidneys have RVs, comma (red) and SBs (dark purple). Both *Six2*$^{PRR-/-}$ and control kidneys show robust UB branching (pink). (D–I) Scale bars= 100 μm.

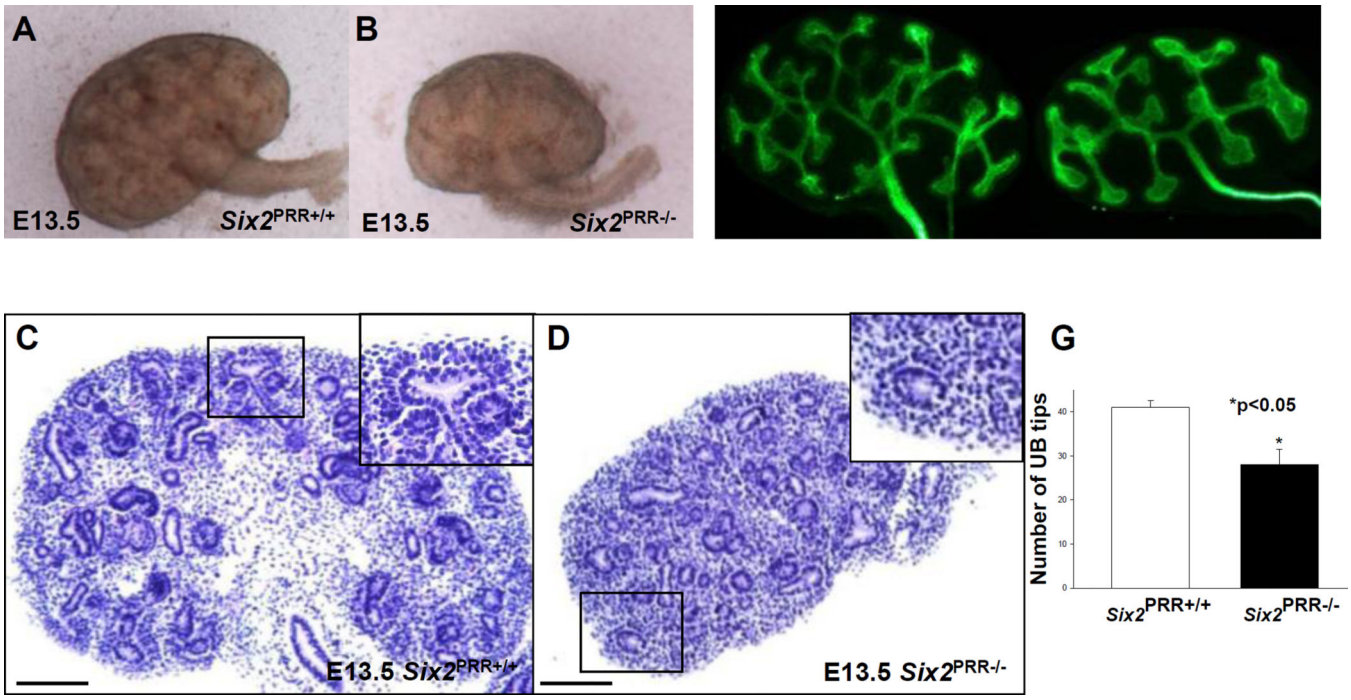

Figure 2. Nephron progenitor PRR is required for normal kidney development

(AD) On E13.5, *Six2*$^{PRR-/-}$ kidneys are reduced in size (A, B) and have less developed epithelial structures on hematoxylin and eosin-stained sections cut in the longitudinal midplane (C, D). Insets in the upper right-hand corners of C and D show higher magnification photos of the respective boxed region. In control kidney (C), nascent vesicle and comma-shaped nephron are observed on ventral surface of branching UB. Mutant kidney is smaller and has no apparent developing nephron structures adjacent to the UB (D, inset). (E–G) The number of UB tips (green staining, anti-pancytokeratin antibody) is reduced in E13.5 mutant compared to control kidneys. (C,D) Scale bars= 100 μm.

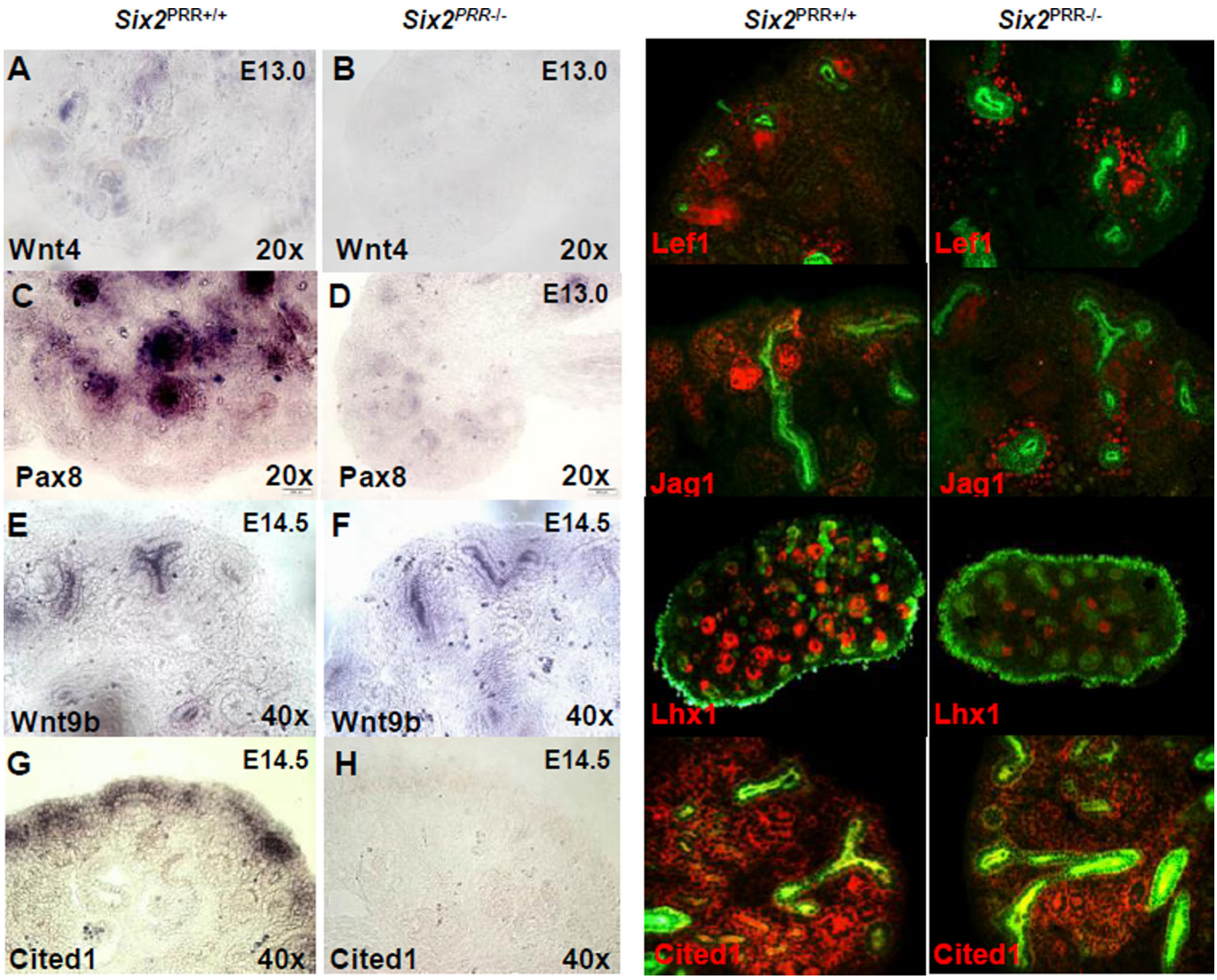

Figure 3. Removal of *PRR* in nephron progenitor cells results in aberrant expression of cap mesenchyme and nephron differentiation markers

(A–H) Section in situ hybridization of nephron induction (*Wnt4, Pax8*), UB (*Wnt9b*) and progenitor cell (*Cited1*) markers in E13.0 (*Wnt4, Pax8*) and E14.5 (*Wnt9b, Cited1*) control and *Six2*$^{PRR-/-}$ kidneys shows reduced *Wnt4Pax8* and *Cited1* expression in mutants, and no apparent change in *Wnt9b*. (I–P) Immunoflurescence for nephron induction markers demonstrates preserved Lef1, Jag1 and Lhx1 expression in control, but decreased formation of pre-tubular aggregates (PTA) and renal vesicles (RV) in *Six2*$^{PRR-/-}$ kidneys on E14.5. Pancytokeratin (I-L, O, P) and calbindin (M, N) (green) label ureteric bud (UB). (O, P) Immunoflurescence for nephron progenitor markers demonstrates preserved Cited1 expression (red) in the cap mesenchyme (CM) in control (O) and decreased expression in *Six2*$^{PRR-/-}$ (P) kidneys

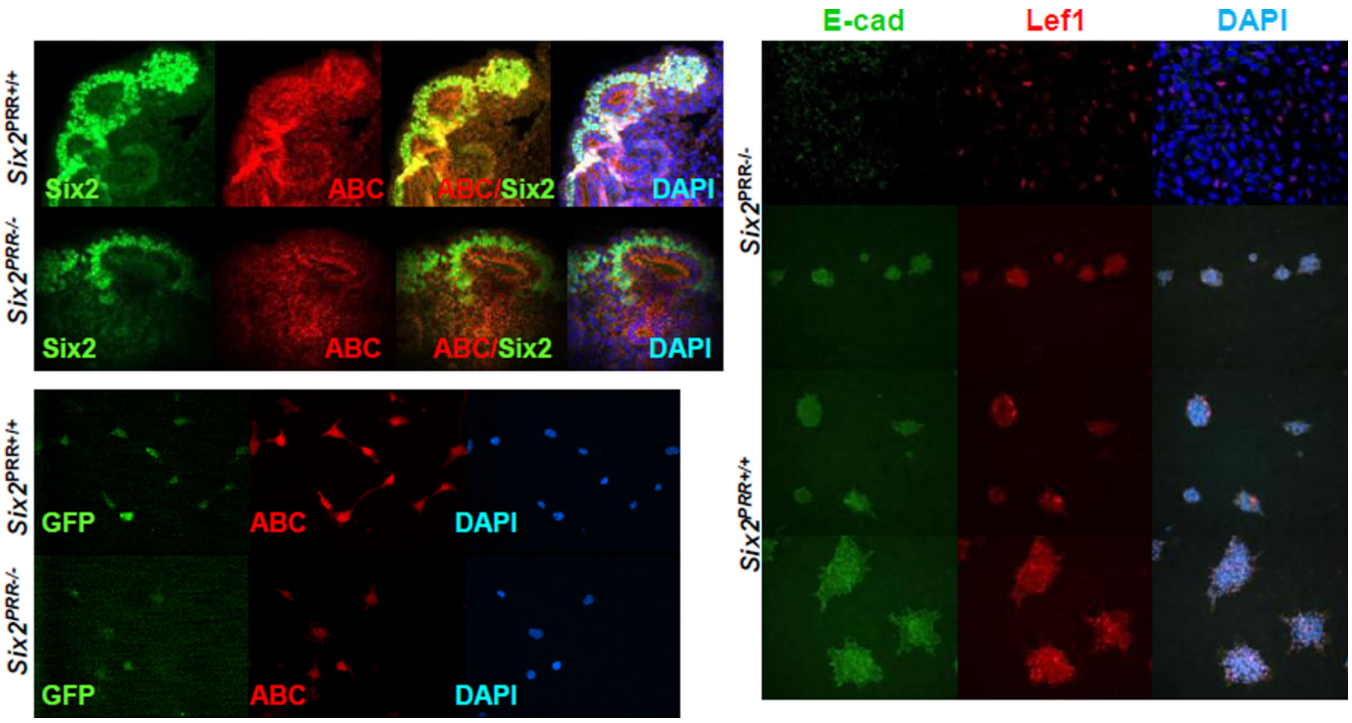

Figure 4. Impaired MET *Six2*$^{PRR-/-}$ compared to control kidneys

(A–H) ABC immunoflurescence shows apparent reduction in ABC levels in the CM of mutant (E–H) compared to control (A–D) E14.5 kidneys. (I–N) Apparent reduction in ABC immunofluorescence (red) in Six2^{+} cells FACS-isolated from E15.5 mutant compared with control kidneys. (O-T') FACS-isolated Six2^{+} cells from E15.5 mutant and wild-type kidneys were pelleted, placed on Transwell membranes and induced to differentiate with 2 μM BIO. (O–Q) DMSO (control)- treated mutant CM cells express less E-cadherin and Lef1, and fail to form complex structures. (O'-Q') Upon stimulation of MET with BIO, induction in E-cadherin and Lef1 expression is attenuated in mutant compared to wild-type cells.

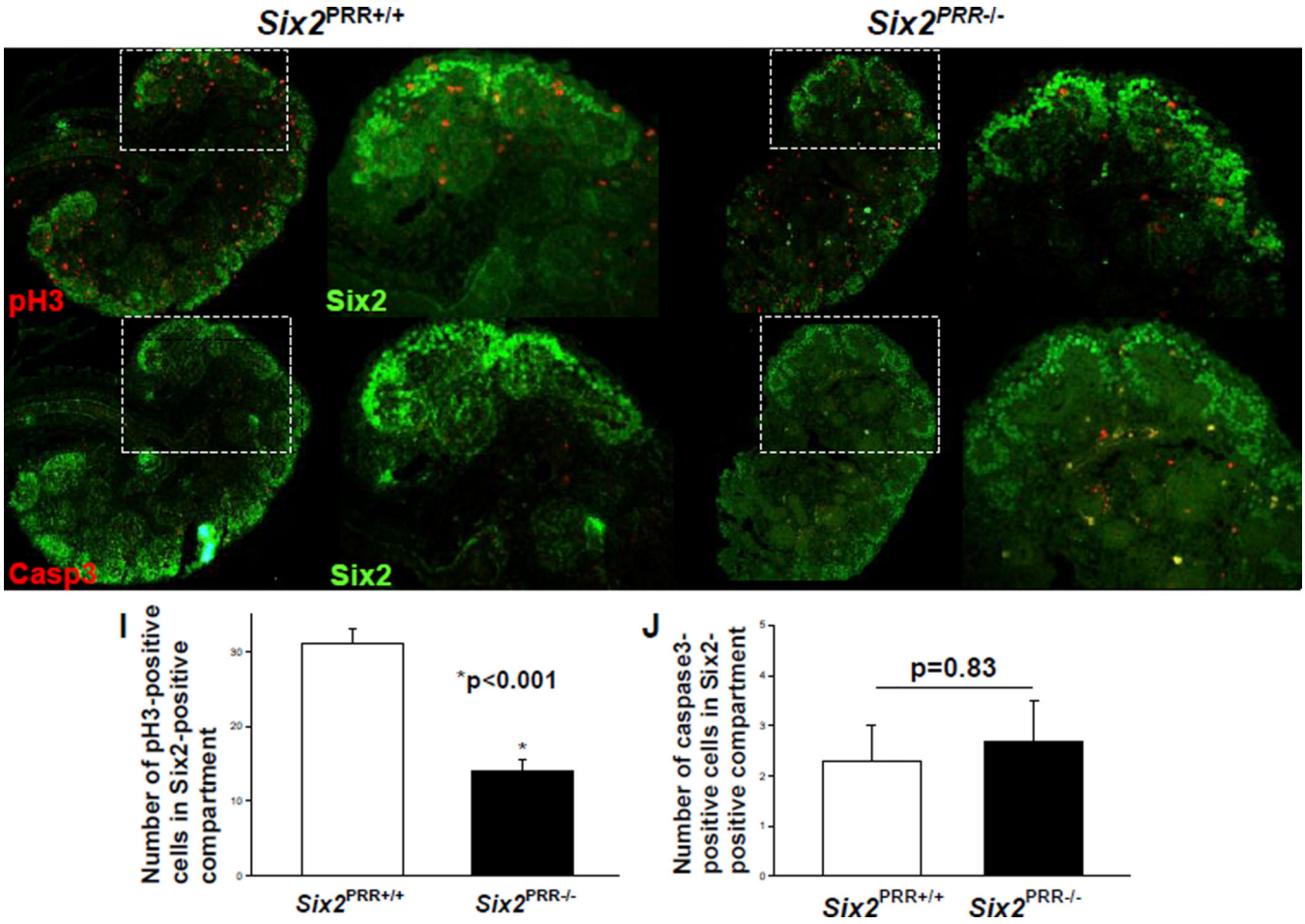

Figure 5. Decreased proliferation and no change in cell death in nephron progenitors in E13.5*Six2*$^{PRR-/-}$ kidneys

(A–H) Immunoflurescence for phospho-histone H3 (pH3), activated caspase-3 (Casp3) (red) and Six2 (green). Representative images demonstrate fewer pH3-positive cells in Six2^{+} compartment of the cap mesenchyme (CM) in *Six2*$^{PRR-/-}$ kidneys than in control littermates. (I,J) Bar graphs show decreased number of pH3-positive cells and no difference in the number of Casp3-positive cells in the CM of *Six2*$^{PRR-/-}$ kidneys compared to controls.

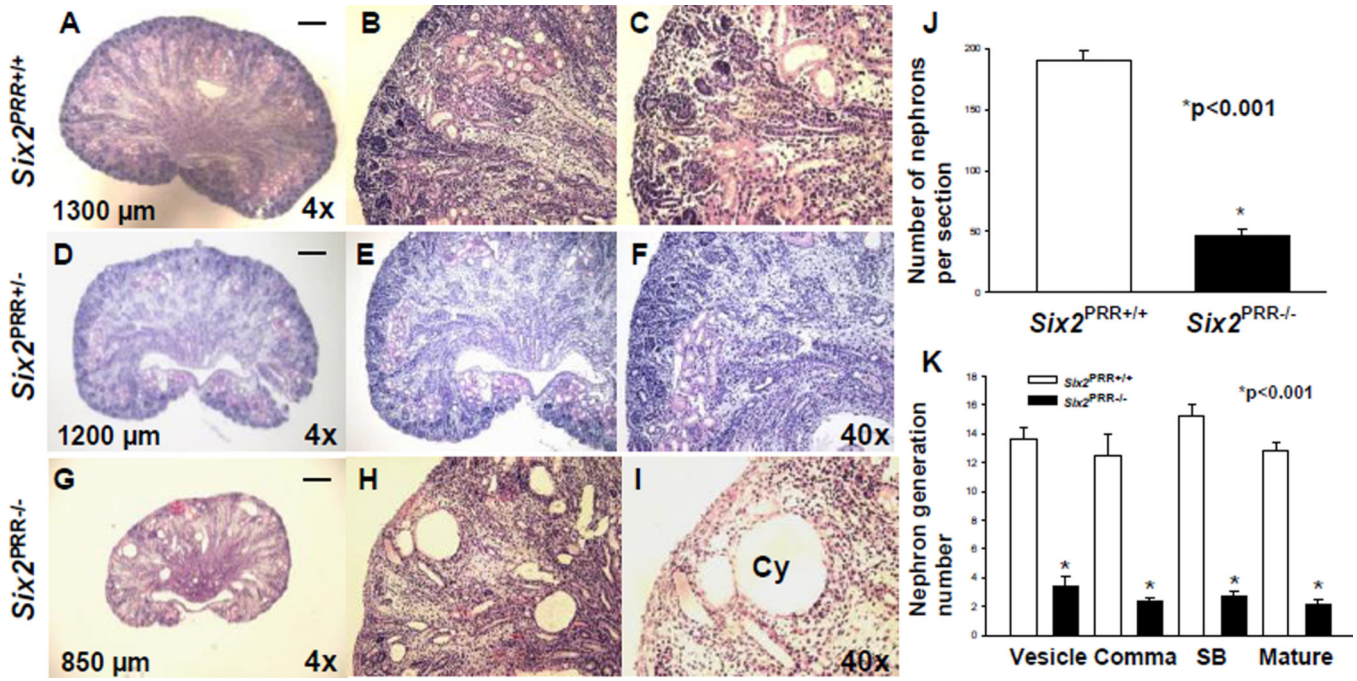

Figure 6. Loss of*PRR* in nephron progenitors results in small cystic kidneys

(A–I) Hematoxylin and eosin-stained sections of P0 kidneys from control (A–C), heterozygous (D–F) and *Six2*$^{PRR-/-}$ (G–I) mice demonstrate reduced kidney size, lack of well-defined nephrogenic zone, thin cortex with apparent reduction in nephron number, presence of cysts (Cy) in the cortex and medulla in *Six2*$^{PRR-/-}$ mutants. (A,D,G) scale bar= 100 μm; numbers- kidney length. (J,K) Bar graphs demonstrate a decrease in total nephron number (J) and in number of all nephron generation stages (K) *Six2*$^{PRR-/-}$ mutants compared to controls.

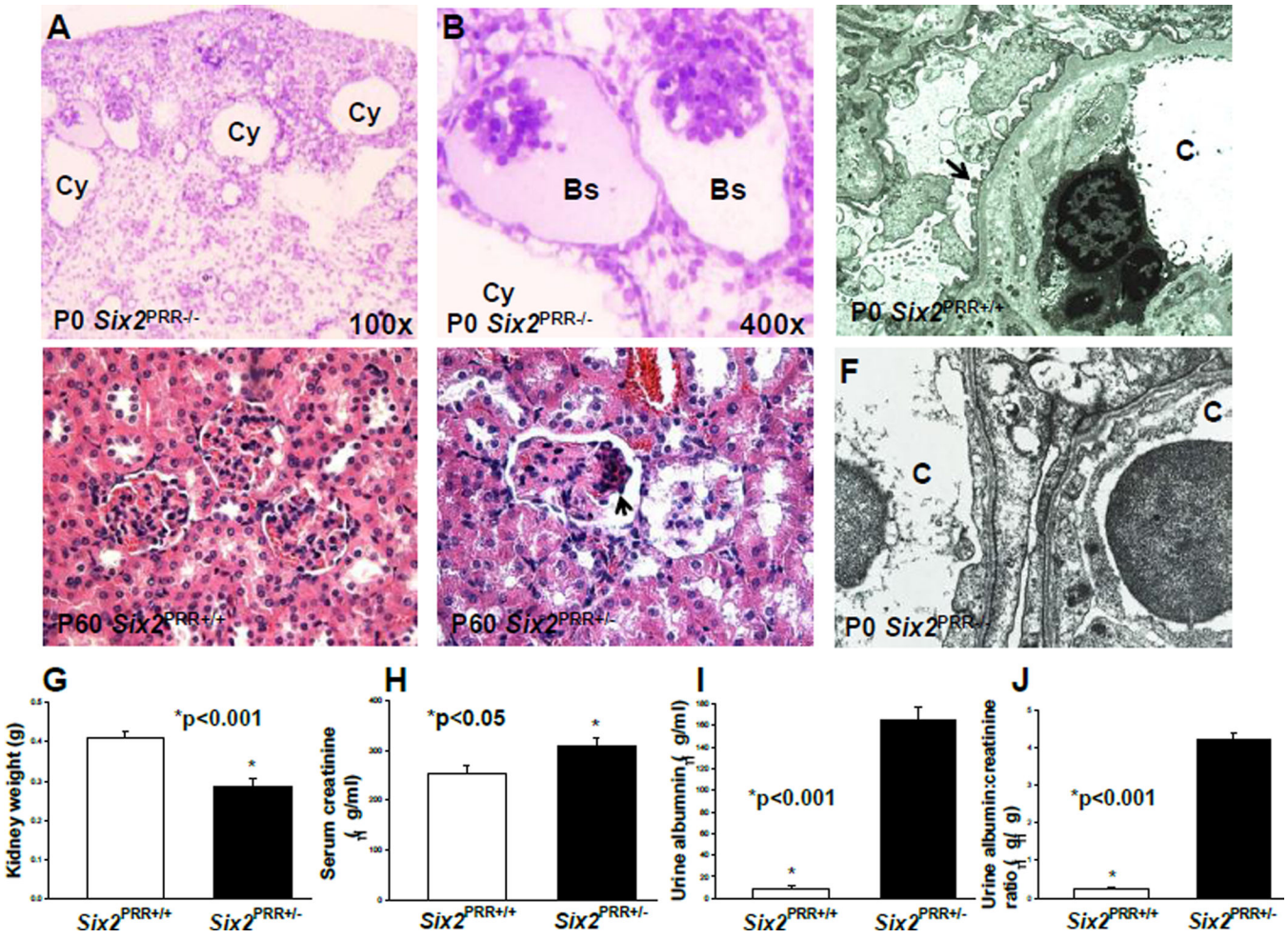

Figure 7. Nephron progenitor*PRR*is required for normal podocyte ultrastructure and kidney function

(A,B) Toluidine blue-stained P0 *Six2*$^{PRR-/-}$ kidney sections show cystically dilated tubules (Cy) and collapsed glomeruli with an enlarged Bowman's space (Bs). (C) Electron micrograph of P0 *Six2*$^{PRR+/+}$ kidney section shows normally appearing podocyte foot processes (arrow). (F) P0 *Six2*$^{PRR-/-}$ kidney section shows fusion and effacement of podocyte foot processes in mutants (arrows); C- capillary lumen (original magnification x20,000). (D–E) Hematoxylin and eosin staining of 2 months-old kidney tissues shows normally appearing glomeruli in *Six2*$^{PRR+/+}$ mice (D) and focal glomerulosclerosis (arrows) in *Six2*$^{PRR+/-}$ mice (E). (G) Kidney weight is reduced in *Six2*$^{PRR+/-}$ compared with *Six2*$^{PRR+/+}$ mice at 2 months of age. (H–J) *Six2*$^{PRR+/-}$ mice have significantly increased levels of serum creatinine, urinary albumin and urinary albumin-to-creatinine ratios at 2 months of age.

Table 1

Mean kidney measurements in E12.5 control and *PRR*$^{UB-/-}$ mice

Parameter	Control (n=3)	Mutant (n=3)	P value
Kidney			
volume (μm^3)	2.64×10^7±4.17×10^6	3.41×10^7±6.63×10^6	0.38
surface area (μm^2)	3.44×105±1.82×104	3.90×105±5.51×104	0.46
Nephron			
developing glomeruli (% of kidney)	3.79±0.01	1.42±0.02	0.001
developing glomeruli average size (μm)	5.1×10^4±2.7×10^3	3.3×10^4±2.4×10^3	0.008
RV number	12.7±2.4	15.6±5.7	0.65
comma number	7.0±1.2	0±0	0.004
SB number	0.43±0.3	0±0	0.04
Ureteric tree			
volume (μm^3)	3.10×10^6±3.47×10^5	4.19×10^6±9.40×10^5	0.33
% of kidney	11.8±0.01	12.2±0.01	0.55
surface area (μm^2)	2.33×10^5±3.01×10^4	3.12×10^5±7.11×10^4	0.36
tip number	29±3	34±8	0.43

Data are expressed as the mean±SE